Automated Soft Contact Lens Detection Using Gradient based Information

Balender Kumar[1] and Aditya Nigam[2] and Phalguni Gupta[3]

[1]*Department of Computer Science and Engineering, Indian Institute of Technology Kanpur (IITK), Kanpur, India*
[2]*School of Computer Science and Electrical Engineering, Indian Institute of Technology Mandi (IIT Mandi), Mandi, India*
[3]*National Institute of Technical Teacher's & Research (NITTTR), Salt Lake, Kolkata, India*
bali@cse.iitk.ac.in, aditya@iitmandi.ac.in, pg@cse.iitk.ac.in

Keywords: Soft Contact Lens, Gradient, Spoofing, Biometric

Abstract: The personal identification number (PIN), credit card numbers and email passwords etc have something in common. All of them can easily be guessed or stolen. Currently, users have been encouraged to create strong passwords by using biometric techniques like fingerprint, palmprint, iris and other such traits. In all biometric techniques, iris recognition can be considered as one of the best, well known and accurate technique but it can be spoofed very easily using plastic eyeballs, printed iris and contact lens. Attacks by using soft contact lens are more challenging because they have transparent texture that can blur the iris texture. In this paper a robust algorithm to detect the soft contact lens by working through a small ring-like area near the outer edge from the limbs boundary and calculate the gradient of candidate points along the lens perimeter is proposed. Experiments are conducted on IIITD-Vista, IIITD-Cogent, UND 2010 and our indigenous database. Result of the experiment indicate that our method outperforms previous soft lens detection techniques in terms of False Rejection Rate and False Acceptance Rate.

1 INTRODUCTION

In such a dynamic and growing world population, human personal authentication using physiological biometric characteristics, can now been seen as a prime social requirement and challenge. There are several well studied traits such as fingerprint, face, iris, ear, palmprint, hand geometry and voice. Since none of them can provide the level of security required/desirable individually, several multimodal systems has also been proposed (Nigam and Gupta, 2015), (Nigam and Gupta, 2014a), (Nigam and Gupta, 2013a) fusing various combinations of palmprint, knuckleprint and iris images in pursuit of superior performance. Image quality can play a very important role in such systems, but it is a very challenging task. Quality can directly effect system performance favorably or adversely. Very limited work is done so far for iris (Nigam et al., 2013), knuckleprint (Nigam and Gupta, 2013b) and palmprint quality estimation as it lacks any such specific texture and structure as compared to face and fingerprints. Some more work on non traditional traits such as knuckleprint and palmprint recognition is reported in (Badrinath et al., 2011), (Nigam and Gupta, 2011), (Nigam and Gupta, 2014b) using SIFT and SURF fusion and $LK-$tracking of corner features.

(a) Transparent Lens   (b) Cosmetic Lens

Figure 1: Type of Contact Lens

Iris is considered as the best available candidate trait for biometric based systems. Flom and Safir (Flom and Safir, 1987) have shown that iris texture is unique for each individual. It has also been proved that iris recognition systems performance degrades when an iris without soft contact lens is compared against same iris with contact lens (Nigam et al., 2015), (Lovish et al., 2015). In this paper we have proposed an algorithm to detect soft contact lens automatically. Contact lenses can be considered as medical devices that can correct your nearsightedness, farsightedness and astigmatism vision problems. Contact lenses have been around for more than four hundred years. First contact lens introduce by Leonardo-da-Vinci in 1505 (71, 2009). In 2004 it was estimated

that 125 million people use contact lenses worldwide (70, 2009). Contact lens can be categorized into two types (i) Transparent contact lens or soft contact lens (ii) Texture contact lens or Cosmetic contact lens. Different types of contact lenses are shown in Figure 1.

Related Work and Background : Detection of cosmetic lens is easier problem as compared to detection of soft contact lens because former has a specific texture present over it. The soft contact lens has no such texture, no color as shown in Figure1. Hence techniques for detecting cosmetic contact lens detection can not be used to detect soft contact lens. In most of the NIR images it is very difficult to detect soft contact lens even by the human eye. But lens boundary is fairly visible because of specular reflection which can be used to identify the contact lens boundary. Algorithm for detection of soft contact and cosmetic contact lenses has been proposed in (Kywe et al., 2006) and the performance of this algorithm is shown in Table1. The algorithm proposed in (Erdogan and Ross, 2013) is based on traditional edge detection exploiting sharp changes in pixel intensity. Performance of this algorithm is also reported in Table1.

	Technique used	Database	Result
(Kywe et al., 2006)	Thermo-Vision	39 Subject	50-66%
(Erdogan and Ross, 2013)	Edge Detection	ICE 2005	72-76%
		MBGC	68.8-70%
(Yadav et al., 2014)	Texture Features	IIITD Cogent	56.66%
		IIITD Vista	67.52%
		UND I(2013)	65.41%
		UND II(2013)	67%

Table 1: Related Work Summary of Soft Contact Lens Detection

2 Proposed Approach

In proposed approach contact lens donat (CLD) is defined and extracted first. Later occlusion is estimated and excluded from contact lens are. Finally Soft Contact Lens Detection (SCLD) algorithm in introduced.

Contact Lens Donat(CLD) : The Contact Lens Donat (CLD) is the area where the possibility of contact lens boundary is assumed to be maximum. It is the part of sclera which lies from CLD_{min} to CLD_{max} as shown in Figure 2 and explained in Section 2.1.

2.1 CLD Detection

In this section, we detect the sclera area where the possibility of contact lens boundary is maximum (in case of contact lens iris image) by moving out radially from the limbus boundary. We call this area as

(a) CLD range   (b) Scan Lines
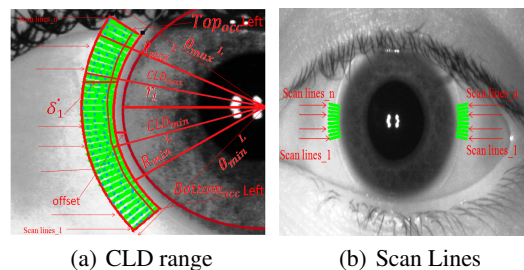
Figure 2: Contact Lens Donat
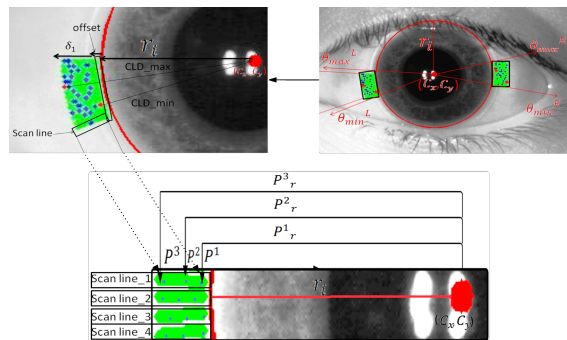
Figure 3: The Angular Range (CLD_{min} and CLD_{max})

contact lens donat which is shown in Figure 2. Detection of contact lens donat has been done by computing the contact lens area limits defined by (CLD_{min} and CLD_{max}) as shown in Figure 3. We have an input iris image I over which we apply segmentation algorithm (Daugman, 1993) and as a result, we get the center (C_x, C_y) and radius r_i of the iris in the input iris image as shown in Figure 2.

(a) NMS for no Lens   (b) NMS for contact Lens
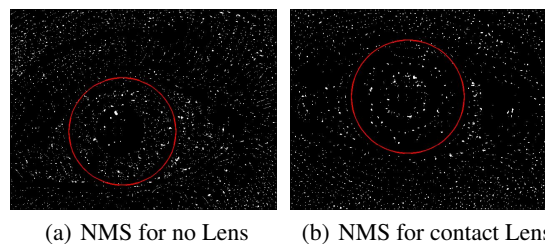
Figure 4: Effect of Non Maximal Suppression(NMS)

2.1.1 Non-Maximal Suppression(NMS) :

Non-maximal suppression is a method to eliminate those points which do not lie in the contact lens boundary. For finding these candidate points, every pixel is compared with its 4 neighboring (left, right, top, bottom) pixels and if the selected pixel is maximum among them, then the corresponding value for that pixel is set to 1, otherwise it is 0 producing a binary image. The figure 4(a) and Figure 4(b) shows

NMS of no lens iris image and soft lens iris image respectively.

2.1.2 Search Range

The maximum possible radial distance for which contact lens donat is present (radial range), can be represented as R_{min} to R_{max} as shown in Figure 2. We define $R_{min} = r_i + offset$ and $R_{max} = R_{min} + \delta$, where $offset$ is a very small constant and δ_1 is the difference between the maximum possible radius of the lens and minimum possible radius of the iris in case of left portion of iris, where radius of contact lens and iris are in *millimeter (mm)*. Similarly δ_2 can be defined for right portion of iris. In general $\delta = \delta_1$ in case of left portion of iris and $\delta = \delta_2$ in case of right portion of iris. But it is observed that for humans, the diameter of the iris lies in the range of 10.2 to 13.0 *mm* and typically it is of *12 mm* (Caroline and Andre, 2002). In case of soft contact lens, the diameter ranges from 13*mm* to 15*mm* (87, 2015). However, diameter of an iris fluctuates from *4 to 8 mm* in the dark and *2 to 4 mm* in bright light (92, 2015). For calculating δ_1 and δ_2, it is assumed that *1 mm* is equivalent to *3.779 pixels*. Ideally δ_1 (in pixels) is equal to 3.779 times of the difference between maximum possible contact lens radius and minimum possible radius of iris but because of dark and bright light effects, some times it may be much more. Exact calculation of δ_1 or δ_2 is difficult because it varies for database to database. We have experimentally found out that it varies from 25 pixels to 35 pixels in the three database that are considered for our study. In ideal condition, $\delta_1 = \delta_2$ as shown in Figure 5(a). But the lens may be misplaced or shifted towards left or right. In case of shifting towards right, δ_2 is greater than δ_1 as shown in Figure 5(b) and in case of shifting towards left δ_1 is greater than δ_2 as shown in Figure 5(c). Here we have fixed value of δ_1, δ_2 experimentally.

Scan lines : These are the radial lines which are orthogonal to the tangent at iris boundary within the range R_{min} to R_{max}. Scan lines are characterized in the region between R_{min} to R_{max} as shown in Figure 2(b). These scan lines are considered at angles ranging from θ_{min} to θ_{max} at an angular distance of $1°$ between two consecutive scan lines, where θ_{min} and θ_{max} are determined experimentally.

With very high possibility, every scan line intersects the lens boundary in case of contact lens images. In Figure 6(a), scan lines are at angles with in the range $[\theta_{min}^L, \theta_{max}^L]$ and $[\theta_{min}^R, \theta_{max}^R]$ where L, R indicates left & right portion of iris. Figure 6(c) shows scan lines in both the regions.

Gradient of each pixel in a scan line is found by using the formula given in Equation 1 and all gradient

(a) Equal   (b) Right Shift   (c) Left Shift
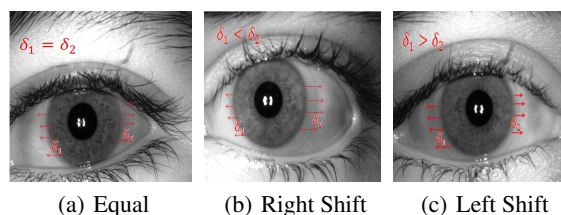
Figure 5: Shifting of Contact Lens

(a) Left Side   (b) Right Side   (c) Both Region
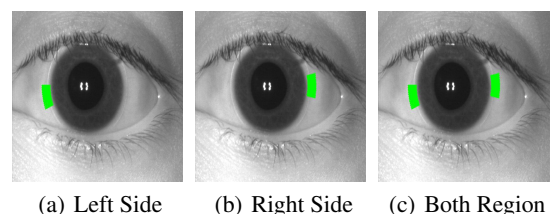
Figure 6: Contact Lens Donat Selected Region

values are stored in an array G.

$$f'(x) = f(x+1) - f(x) \qquad (1)$$

Three absolute maximum gradient pixels from G which are locally maximum are extracted. Non-maximal suppression preserves local maximal property. This process is repeated for each scan line. In Figure 7, blue points indicate maximum gradient pixels in each scan line. Three maximum gradient pixels (*viz.* P^1, P^2, P^3) are considered because if only one maximum intensity pixel is selected, then there is a possibility that it is an outlier due to illumination effects, eyelid-eyelashes etc.

(a) Left   (b) Right   (c) Both
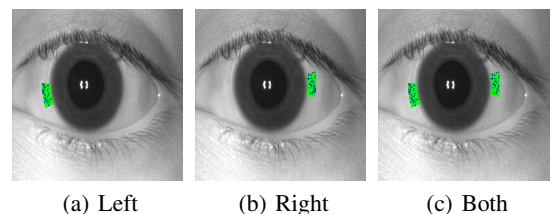
Figure 7: Three Maximum Intensity Pixel in Each line

Corresponding to these three maximum intensity pixels for each scan line their distances from the center of the iris are stored and these distances are denoted as P_r^1, P_r^2 and P_r^3, where θ denotes the number of scan lines. The minimum and maximum distances from the selected pixel are denoted as CLD_{min} and CLD_{max} respectively. In Figure 3, red points show pixel values corresponding to CLD_{min} and CLD_{max}.

2.2 Occlusion Exclusion from Lens

Eyelids and eyelashes are two major challenges in contact lens detection. There is a need to detect them

initially because eyelashes cover some part of the contact lens and due to which, the intensity varies, that in turn, many affect the accuracy of the proposed lens detection algorithm. Eyelids must also be detected early as once can assume that lens cannot be beyond the eyelid boundaries. So detection of eyelid helps to set dynamic angle range which depends on the visibility of contact lens. The *False Acceptance Rate(FAR)* and *False Rejection Rate(FRR)* increases sharply if eyelid and eyelashes are not detected correctly.

We have proposed a novel approach for occlusion exclusion from contact lens area. We detect the occlusion from contact lens area using an edge detection algorithm. It is assumed that over sclera, there cannot be very prominent edge points (with higher threshold). If some edges are present on sclera they must be due to eyelashes and eyelids. Hence using these edge points, we define our angle range which is dynamic in nature. Therefore, use of eyelid can ensure that our algorithm never crosses the eyelid boundaries.

Given any iris image I as input similar to the one shown in Figure 8(a) segmentation algorithm is applied on I to obtain the iris center as (C_x,C_y) and the distance from center to limbus boundary r_i. In the first step of the algorithm, we generate an edge map of iris image on higher threshold. False edges are expelled by removing those connected components which are less than P pixels and a binary image is obtained with no false edge as shown in Figure 8(b).

(a) Original Image (b) Edge Map
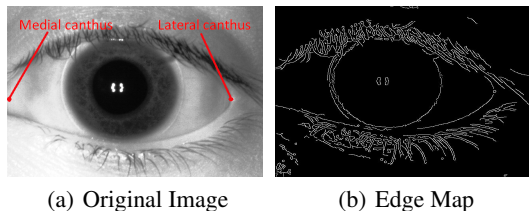
Figure 8: Generating edge map of original image

In the next step, scan lines are characterized in the range of R_{min}^L to R_{max}^L where $R_{min}^L=(r_i + \delta_1 +offset)$ and $R_{max}^L=(R_{min}^L + \delta_3)$ for left portion of iris and R_{min}^R to R_{max}^R where $R_{min}^R=(r_i + \delta_2 +offset)$ and $R_{max}^R=(R_{min}^R + \delta_4)$ for right portion of iris on the iris edge map, where δ_1 and δ_2 are the same as explained in Section 2.1.2. But values of δ_3 and δ_4 depend on visible part of contact lens and are selected experimentally. We can set $offset \geq 0$ with δ_3, $\delta_4 \in [1,10]$. If δ_3, δ_4 are greater then 10, there is a possibility that angle is shrinking as medial canthus or lateral canthus are reached as shown in Figure 8(a) that can degrade the accuracy of the proposed algorithm. These scan lines are at angles ranging from θ_{min}^L to θ_{max}^L for left portion of iris image and θ_{min}^R to θ_{max}^R for right portion of iris with $1°$ angular distance between two consecu-

tive scan lines. Figure 9 shows the objective region secured by the scan lines. In Figure 9(a) and Figure 9(b), scan lines are extracted from left and right portion of iris image respectively where as Figure 9(c) shows the union of both.

(a) (b) (c)
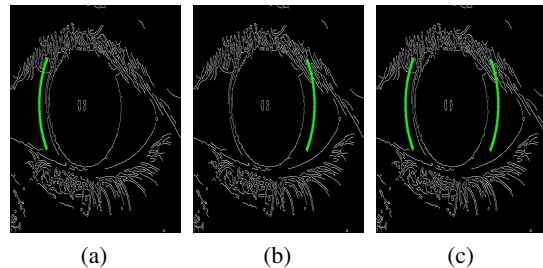
Figure 9: Eyelashes and Eyelid limits

Scan line over sclera, has very few non-zero (edge) pixels. On the other side if the current scan line intersects eyelashes or eyelids then with very high probability non-zero (edge) pixels are found. For each scan line at an angle θ, the number of non-zero pixels is counted. If the count of non-zero pixels is greater than threshold T then a value 1 is set to $H(\theta)$ array, otherwise value 0 is stored in $H(\theta)$, where θ represents the number of scan lines. This process is repeated for all scan lines.

(a) Left portion (b) Right portion (c) Union of both
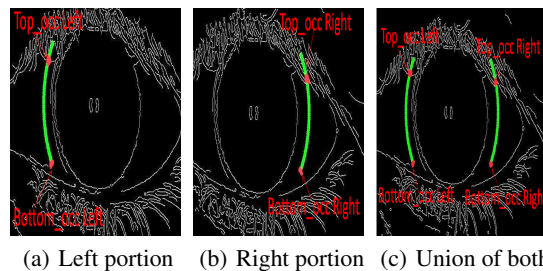
Figure 10: Occlusion estimation [$Bottom_{occ},Top_{occ}$]

In order to estimate top and bottom occlusion angles, two maximal (in terms of angular distance) scan-lines between which all scan-lines are having their edge pixels less than T (i.e not occluded) in $H(\theta)$ are found. The lower index angle is called $Bottom_{occ}$ which represents lower eyelid or eyelash and the higher index angle is called Top_{occ} which represents the upper eyelid or eyelashes. In Figure 10, a lower red line indicates the $Bottom_{occ}$ and upper red line indicates the Top_{occ}.

2.3 Soft Contact Lens Detection (SCLD)

In this section we explain the feature extraction of the iris image on the basis of which one can determines whether it is a contact lens iris or no lens iris. The

detailed description of feature encoding is shown in Figure 11. The proposed algorithm starts with denoising the image. The motivation behind denoising iris image is to reduce the noise & and preserve iris features. Top-Hat filtering is applied on the iris image to reduce uneven illumination effect because it reduces the accuracy of the system.

(a)
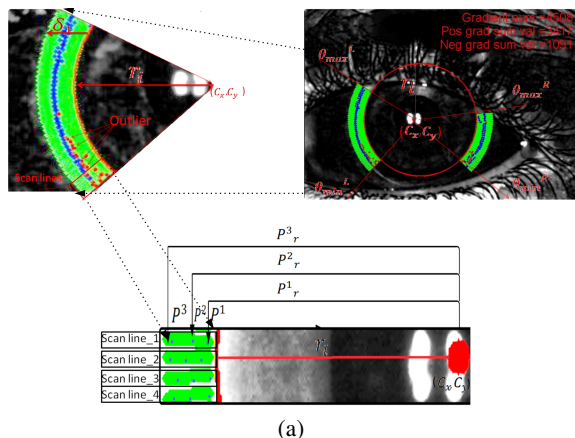
Figure 11: SCLD using Gradient

(a) No Lens

(b) Top hat filtering result

(c) Soft Lens

(d) Top hat filtering result
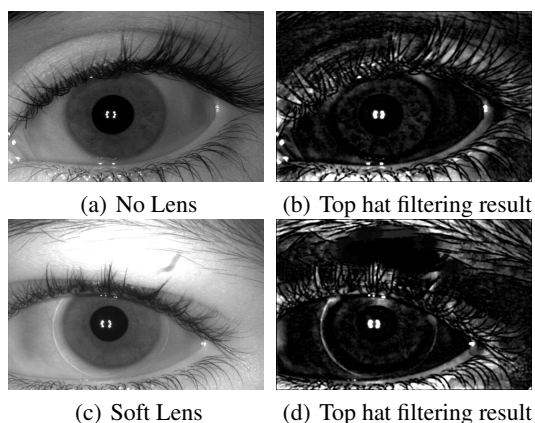
Figure 12: Top Hat Filtering Effect

Non maximal-suppression (NMS) algorithm is applied to predict and remove false edges. Scan lines are characterized with in the search range explained in Section 2.1.2 and result is shown in Figure 13. Angular Range for these scan lines is also explained previously. The parameter CLD_{min}, CLD_{max} and $Bottom_{occ}$, Top_{occ} are calculated separately for left and right part of the iris.

Scan lines satisfying the condition are extracted from the considered region defined as: they must lie with in the radial range CLD_{min} to CLD_{max} with an angular range $Bottom_{occ}$ to Top_{occ} as shown as in Figure 14 for no lens and in Figure 15 for soft lens.
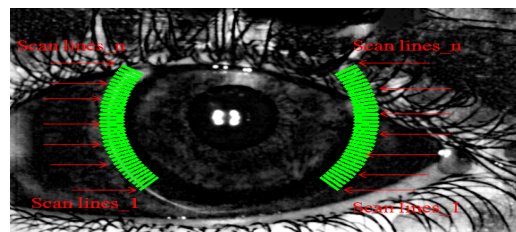
Figure 13: Scan Lines Arrangement

(a) Left region   (b) Right region   (c) Union of both

Figure 14: Region after Occlusion Exclusion (No Lens)

(a) Left region   (b) Right region   (c) Union of both

Figure 15: Region after Occlusion Exclusion (Soft Lens)

Each scan line has high probability to intersect contact lens boundary (if belonging to contact lens class). The gradient of each pixel in a scan line is calculated using Equation 1 and stored in an array G. In a scan line we extract three absolute maximum gradient pixels from G which are locally maximum with their pixel intensity more than t. The value t is the pixel intensity threshold ensuring that any value less than t, must be excluded from contact lens boundary. This process is repeated for each scan line. These three maximum gradient pixels are considered because selecting only one maximum gradient pixel may result in an outlier selection, due to uneven illumination. In Figures 16, 17, blue points indicate the selected maximum intensity pixels and red points indicate the outlier in scan lines for no lens & soft lens iris image respectively. These points depend on images.

An outlier can be seen as an extremely high or low value in the stored gradient pixels. For remaining gradient pixels, we maintain three separate accumulator (sum of gradient pixels) *viz.* $G1$, $G2$ and $G3$ for positive and negative and absolute gradient values. These values form a feature vector that later has been used to detect the contact lens. The positive, negative and absolute gradient sums are marked in Figure 18 and Figure 19 for no lens & soft lens iris image. The pro-
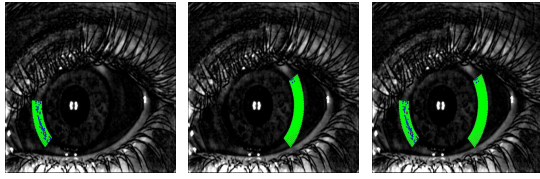
(a) Left region   (b) Right region   (c) Union of both

Figure 16: Largest Gradient Pixel (No Lens)

cess flow diagram to find out gradient sums from each iris images is shown in Figure 20.
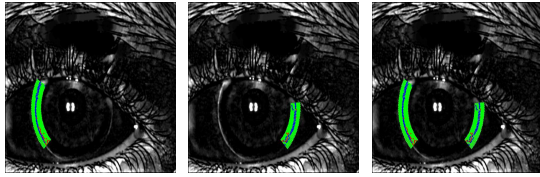
(a) Left region   (b) Right region   (c) Union of both

Figure 17: Largest Gradient pixel (Soft Contact Lens)
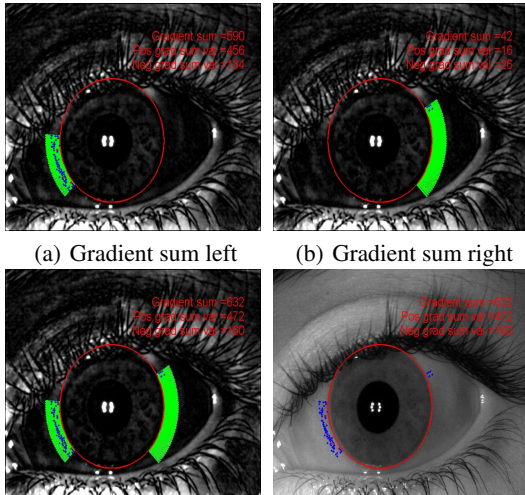
(a) Gradient sum left   (b) Gradient sum right

(c) Gradient sum union   (d) Original image

Figure 18: Gradient Pixel Sum (No Lens)

3 Experimental Section

Dataset : Three diverse publicly available database are utilized to evaluate the performance of soft contact lens detection system viz IITK , IIITD (Yadav et al., 2014; Kohli et al., 2013) and UND Contact lens database. All databases are acquired using different iris sensors like FA2, LG 4000. All three databases contain iris images in three situations: (a)
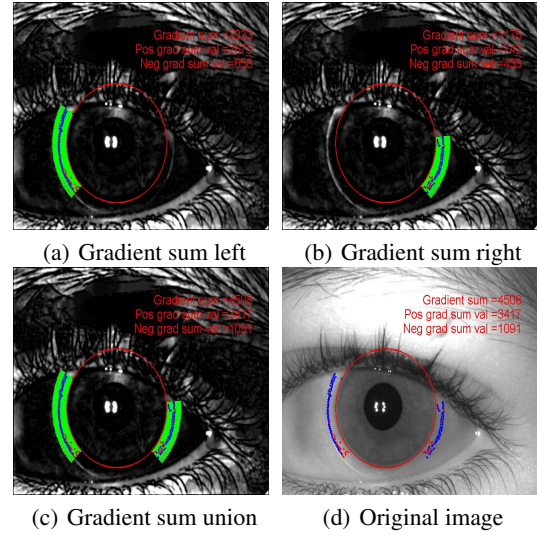
(a) Gradient sum left   (b) Gradient sum right

(c) Gradient sum union   (d) Original image

Figure 19: Gradient Pixel Sum (Soft Lens)
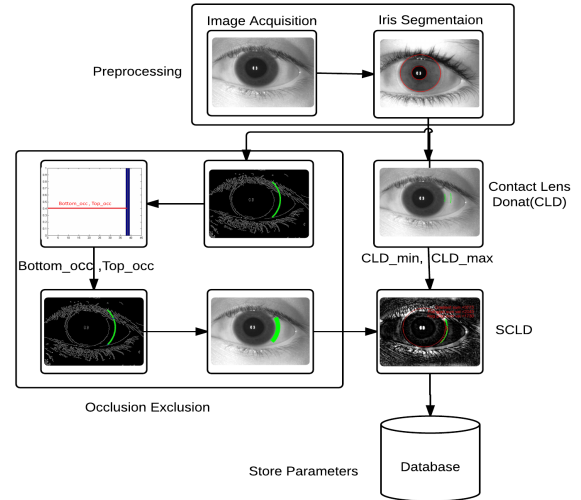
Figure 20: Overview of SCLD algorithm using Gradient

Iris image with soft contact lens ['Y'], (b) Iris image with color lens ['C'], (c) Iris image with no lens ['N']. In this paper we have focused on soft contact lens detection hence only ['N','Y'] classes are taken into consideration to test our system.

Database division into Left and Right eye : It is observed that most of the databases are collected by considering only single iris at a time using NIR camera. While capturing left iris it is observed that more light falls on right side of left iris. This infer that left iris image has more visible lens part on its right side as shown in Figure 21(a) and vice-versa as shown in Figure 21(b). Another observation is that θ range and r range depends on database but can be fixed for any individual database.

(a) Left Iris Image	(b) Right Iris Image
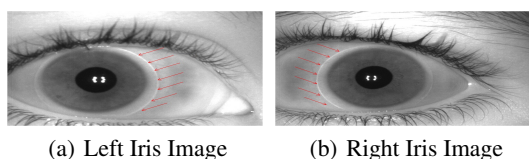
Figure 21: Visibility of Soft Contact Lens

Threshold Selection : Every dataset is divided into two part with 66% being utilized for computing feature value threshold and remaining for testing purpose. In order to find the best suitable threshold over this training data, all possible threshold in the range $\{0 \text{ to } 1\}$ are tested. The threshold (say T_{best}) at which the system performance got maximized is used for testing.

Prediction : The remaining 34% of the dataset is used for testing. Again normalized feature values are computed and compared with the above computed threshold T_{best}. If the calculated normalized feature value is greater than or equal to the T_{best} then that sample is marked as lens, otherwise it is marked as no lens.

Descriptor	SCLD using Gradient				
Database	CCR	Accuracy	FAR	FRR	EER
Our Database Left Eye	**85.92**	84.99	15.41	16.52	15.96
Our Database Right Eye	82.40	82.62	20.59	14.15	17.37
IIITD Vista Left Eye	84.47	84.43	16.62	14.66	15.64
IIITD Vista Right Eye	86.05	85.86	13.11	17.63	15.37
IIITD Cogent Left Eye	80.52	80.70	18.89	21.66	20.28
IIITD Cogent Right Eye	84.99	80.46	18.4676	20.60	19.53
UND	83.24	83.31	17.28	19.60	18.44

Table 2: CCR, Accuracy, FAR, FRR and EER across Various databases

The comparative performance analysis for the proposed system in terms EER and accuracy for different databases is shown in Table2 and in Figures 22, 23. To best of our knowledge this can be considered as an earliest work detecting only soft contact lens on IIITD Vista, IIITD Cogent and UND database.

4 Limitation of the system

Some limitation that can also be seen as a future work of the proposed algorithm are stated below.

[i] Defocused and Blurred Images : Defocus is the variation in which a picture is essentially out of core interest. This happens because of lens deviate from accurate focus. There may also be blurring due to defocus or movement of the lens. Some defocused and blurred images are shown in Figure 24(a). Our algorithm failed in such cases because lens edges are not properly visible.

[ii] Shifted Lens toward Upper or Lower Eyelid : For data collection purposes, subject has to wear contact lens. For individuals who have never used contact lenses earlier found it difficult to wear it correctly and end up with shifted lens problem. In the proposed algorithm we handle the lateral move *i.e.* shifting towards lateral canthus and medial canthus. However algorithm fails if shifting occurs toward upper or lower eyelid as shown in the Figure 24(b).

[iii] Sleepy Eye : In such cases contact lens faintly visible causing algorithm to fail. Some images are shown in the Figure 24(c).

REFERENCES

(2009). A Brief History of Contact Lenses. http://www.contactlenses.org/timeline.htm. Accessed: 2015-04-27.

(2009). Contact lens. http://en.wikipedia.org/wiki/Contact_lens. Accessed: 2015-04-27.

(2015). Soft Contact Lens Diameter. http://softspecialedition.com/base_curve. Accessed: 2015-5-13.

(2015). The Pupils. http://www.ncbi.nlm.nih.gov/books/NBK381/. Accessed: 2015-06-12.

Badrinath, G., Nigam, A., and Gupta, P. (2011). An efficient finger-knuckle-print based recognition system fusing sift and surf matching scores. In Qing, S., Susilo, W., Wang, G., and Liu, D., editors, *Information and Communications Security*, volume 7043 of *Lecture Notes in Computer Science*, pages 374–387. Springer Berlin Heidelberg.

Caroline, P. and Andre, M. (2002). The effect of corneal diameter on soft lens fitting, part 2. *Contact Lens Spectrum*, 17(5):56–56.

Daugman, J. (1993). High confidence visual recognition of persons by a test of statistical independence. *IEEE Transactions on Pattern Analysis and Machine Intelligence*, 15(11):1148–1161.

Erdogan, G. and Ross, A. (2013). Automatic detection of non-cosmetic soft contact lenses in ocular images. In *SPIE Defense, Security, and Sensing*, pages 87120C–87120C. International Society for Optics and Photonics.

Flom, L. and Safir, A. (1987). Iris recognition system. US Patent 4,641,349.

Kohli, N., Yadav, D., Vatsa, M., and Singh, R. (2013). Revisiting iris recognition with color cosmetic contact lenses. In *Proceedings of International Conference on Biometrics (ICB)*, pages 1–7. IEEE.

Kywe, W. W., Yoshida, M., and Murakami, K. (2006). Contact lens extraction by using thermo-vision. In *Pattern Recognition, 2006. ICPR 2006. 18th International Conference on*, volume 4, pages 570–573. IEEE.

Lovish, Nigam, A., Kumar, B., and Gupta, P. (2015). Robust contact lens detection using local phase quantiza-

(a) Equal Error Rate   (b) Accuracy   (c) CCR
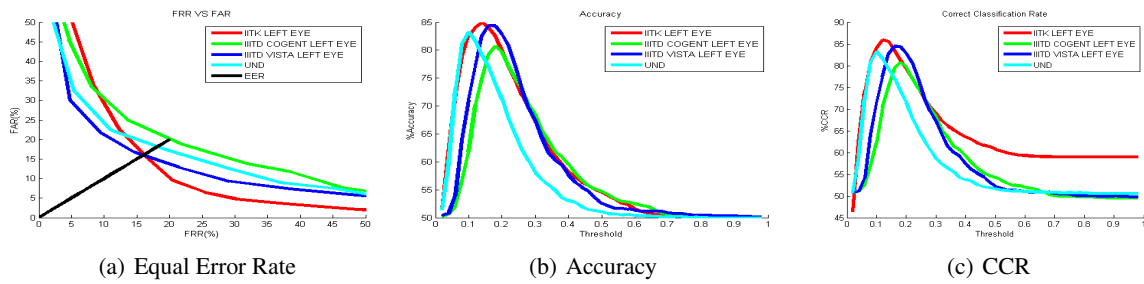
Figure 22: SCLD using Gradient Performance Comparison for various Left Eye Database

(a) Equal Error Rate   (b) Accuracy   (c) CCR
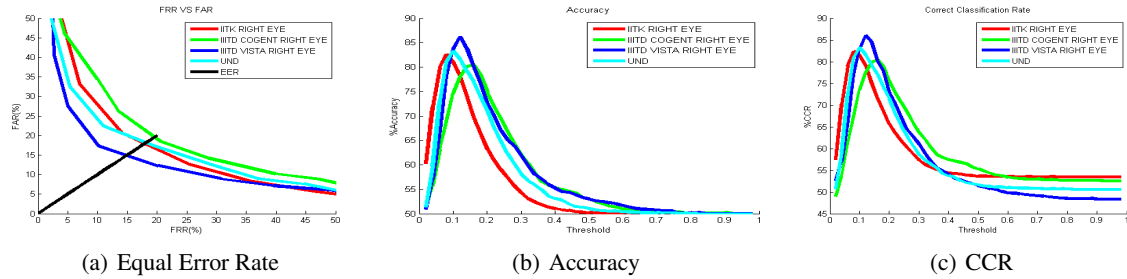
Figure 23: SCLD using Gradient Performance Comparison on various Right Eye Database

(a) Defocused and Blurred   (b) Shifted Lens   (c) Sleepy Eye
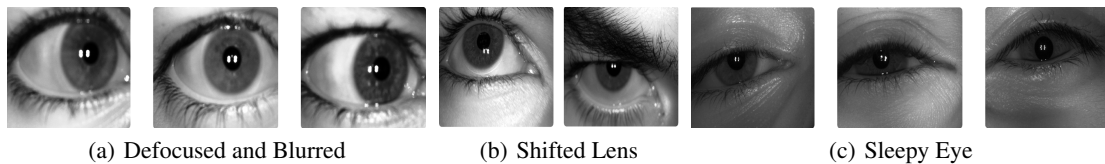
Figure 24: Limitation of the system

tion and binary gabor pattern. In *Computer Analysis of Images and Patterns*, volume 9256, pages 702–714.

Nigam, A. and Gupta, P. (2011). Finger knuckleprint based recognition system using feature tracking. In Sun, Z., Lai, J., Chen, X., and Tan, T., editors, *Biometric Recognition*, volume 7098 of *Lecture Notes in Computer Science*, pages 125–132. Springer Berlin Heidelberg.

Nigam, A. and Gupta, P. (2013a). Multimodal personal authentication system fusing palmprint and knuckleprint. In Huang, D.-S., Gupta, P., Wang, L., and Gromiha, M., editors, *Emerging Intelligent Computing Technology and Applications*, volume 375 of *Communications in Computer and Information Science*, pages 188–193. Springer Berlin Heidelberg.

Nigam, A. and Gupta, P. (2013b). Quality assessment of knuckleprint biometric images. In *Image Processing (ICIP), 2013 20th IEEE International Conference on*, pages 4205–4209.

Nigam, A. and Gupta, P. (2014a). Multimodal personal authentication using iris and knuckleprint. In Huang, D.-S., Bevilacqua, V., and Premaratne, P., editors, *Intelligent Computing Theory*, volume 8588 of *Lecture Notes in Computer Science*, pages 819–825. Springer International Publishing.

Nigam, A. and Gupta, P. (2014b). Palmprint recognition using geometrical and statistical constraints. In Babu, B. V., Nagar, A., Deep, K., Pant, M., Bansal, J. C., Ray, K., and Gupta, U., editors, *Proceedings of the Second International Conference on Soft Computing for Problem Solving (SocProS 2012), December 28-30, 2012*, volume 236 of *Advances in Intelligent Systems and Computing*, pages 1303–1315. Springer India.

Nigam, A. and Gupta, P. (2015). Designing an accurate hand biometric based authentication system fusing finger knuckleprint and palmprint. *Neurocomputing*, 151, Part 3:1120 – 1132.

Nigam, A., Kumar, B., Triyar, J., and Gupta, P. (2015). Iris recognition using discrete cosine transform and relational measures. In *Computer Analysis of Images and Patterns*, volume 9257, pages 506–517.

Nigam, A., T., A., and Gupta, P. (2013). Iris classification based on its quality. In Huang, D.-S., Bevilacqua, V., Figueroa, J., and Premaratne, P., editors, *Intelligent Computing Theories*, volume 7995 of *Lecture Notes in Computer Science*, pages 443–452. Springer Berlin Heidelberg.

Yadav, D., Kohli, N., Doyle, J., Singh, R., Vatsa, M., and Bowyer, K. W. (2014). Unraveling the effect of textured contact lenses on iris recognition. *IEEE Transactions on Information Forensics and Security*.